



**HESSD**

11, 9643–9669, 2014

**Prediction of extreme  
floods based on  
CMIP5 climate  
models**

C. H. Wu et al.

This discussion paper is/has been under review for the journal Hydrology and Earth System Sciences (HESS). Please refer to the corresponding final paper in HESS if available.

# Prediction of extreme floods based on CMIP5 climate models: a case study in the Beijiang River basin, South China

C. H. Wu<sup>1</sup>, G. R. Huang<sup>1,2</sup>, and H. J. Yu<sup>1</sup>

<sup>1</sup>School of Civil Engineering and Transportation, South China University of Technology, Guangzhou 510640, China

<sup>2</sup>State Key Laboratory of Subtropical Building Science, South China University of Technology, Guangzhou 510640, China

Received: 4 August 2014 – Accepted: 6 August 2014 – Published: 13 August 2014

Correspondence to: G. R. Huang (huanggr@scut.edu.cn)

Published by Copernicus Publications on behalf of the European Geosciences Union.

Title Page

Abstract

Introduction

Conclusions

References

Tables

Figures



Back

Close

Full Screen / Esc

Printer-friendly Version

Interactive Discussion



## Abstract

The occurrence of climate warming is unequivocal, and is expected to be experienced through increases in the magnitude and frequency of extreme events, including flooding. This paper presents an analysis of the implications of climate change on the future flood hazard in the Beijiang River basin in South China, using a Variable Infiltration Capacity (VIC) model. Uncertainty is considered by employing five Global Climate Models (GCMs), three emission scenarios (RCP2.6, RCP4.5, and RCP8.5), ten downscaling simulations for each emission scenario, and two stages of future periods (2020–2050, 2050–2080). Credibility of the projected changes in floods is described using an uncertainty expression approach, as recommended by the Fifth Assessment Report (AR5) of the Intergovernmental Panel on Climate Change (IPCC). The results suggest that the VIC model shows a good performance in simulating extreme floods, with a daily runoff Nash and Sutcliffe efficiency coefficient (NSE) of 0.91. The GCMs and emission scenarios are a large source of uncertainty in predictions of future floods over the study region, although the overall uncertainty range for changes in historical extreme precipitation and flood magnitudes are well represented by the five GCMs. During the periods 2020–2050 and 2050–2080, annual maximum 1-day discharges (AMX1d) and annual maximum 7-day flood volumes (AMX7fv) are projected to show very similar trends, with the largest possibility of increasing trends occurring under the RCP2.6 scenario, and the smallest possibility of increasing trends under the RCP4.5 scenario. The projected ranges of AMX1d and AMX7fv show relatively large variability under different future scenarios in the five GCMs, but most project an increase during the two future periods (relative to the baseline period 1970–2000).

# HESSD

11, 9643–9669, 2014

## Prediction of extreme floods based on CMIP5 climate models

C. H. Wu et al.

Title Page

Abstract

Introduction

Conclusions

References

Tables

Figures

⏪

⏩

◀

▶

Back

Close

Full Screen / Esc

Printer-friendly Version

Interactive Discussion







## 2 Data and methodology

### 2.1 Study area

The study area called the Feilaixia catchment is located in the upstream of the Beiji-  
5 River (Fig. 1). It has a drainage area of 34 097 km<sup>2</sup> and accounts for 73 % of the Bei-  
jiang River basin. The Feilaixia catchment consists of four main tributaries, the Wujiang  
River, Zhenjiang River, Lianjiang River and Wengjiang River (Fig. 1). The region is an  
important water source for the Guangdong province, one of the most developed areas  
of China. The climate of the region is warm wet tropical to subtropical, and precipita-  
10 tion during the flood season (April to September) accounts for 70–80 % of the annual  
precipitation. Location of hydro-meteorological stations used in the study is shown in  
Fig. 1.

### 2.2 Datasets

Data used in this study include digital elevation model (DEM), vegetation cover, soil  
15 properties, and observed hydro-meteorological data. The DEM (at a resolution of  
90 m) was derived from the International Scientific & Technical Data Mirror Site, Com-  
puter Network Information Center, Chinese Academy of Sciences. Vegetation cover-  
age datasets were collected from the University of Maryland (UMD), and provide in-  
formation on global land classification at a 1 km resolution (Hansen et al., 2000). The  
20 classification of soil texture at a resolution of 1 km based on the Harmonized World  
Soil Database (HWSD) was provided by the Food and Agriculture Organization of  
the United Nations (FAO) and the International Institute for Applied Systems Analy-  
sis (IIASA).

Daily hydrological data as recorded at 27 rainfall stations and 1 discharge station  
25 were provided by the Hydrology Bureau of the Guangdong Province, China. Daily max-  
imum and minimum temperature data from 4 stations were provided by Meteorological  
Data Sharing Service System, National Meteorological Information Center, China Me-

HESSD

11, 9643–9669, 2014

## Prediction of extreme floods based on CMIP5 climate models

C. H. Wu et al.

Title Page

Abstract

Introduction

Conclusions

References

Tables

Figures

⏪

⏩

◀

▶

Back

Close

Full Screen / Esc

Printer-friendly Version

Interactive Discussion



teorological Administration (<http://cdc.cma.gov.cn/home.do>). The data sets from all the stations spanned over the period from 1969 to 2011.

## 2.3 CMIP5 climate models

CMIP5 is the Coupled Model Intercomparison Project Phase 5, which provides a framework for coordinated climate change experiments for the next several years, and thus includes simulations for assessment in the AR5, as well as for others that extend beyond the AR5 (Taylor et al., 2012). Relative to earlier phases, CMIP5 focuses on a set of experiments that include higher spatial resolution models, improved model physics, and a richer set of output fields (Gulizia and Camilloni, 2014; Taylor et al., 2012). Additionally, the CMIP5 climate change projections are driven by new climate scenarios that use a time series of emissions and concentrations from the representative concentration pathways (RCPs) described in Moss et al. (2010). Accordingly, GCMs provided by the CMIP5 have been widely used in the assessment of climate change (Gulizia and Camilloni, 2014; Pierce et al., 2013; Smith et al., 2013).

When using multiple GCMs to assess future climate change, the underlying assumption is that different models provide statistically independent information. In fact, models usually share physical parameterization schemes, and at times, even large parts of the same code (Pincus et al., 2008), which could lead to similar weaknesses among the models. Pennell and Reichler (2011) evaluated 24 state-of-the-art models of the CMIP3 and their ability to simulate broad aspects of twentieth-century climate, and found that the effective number of models (the amount of statistically independent information in the simulations) was significantly less than the actual number of models. Xiao et al. (2013) applied the Hierarchical Cluster Analysis (HCA) to analyse the precipitation simulation similarity of 47 CMIP5 GCMs over the Zhujiang River basin, and suggested that the 47 GCMs can be classified into five types.

According to Xiao et al. (2013), 5 CMIP5 GCMs (i.e. BCC-CSM1.1, CanESM2, CSIRO-Mk3.6.0, GISS-E2-R, and MPI-ESM-LR), which are independent from each other and have a good performance in current climate simulation for the Zhujiang River

# HESSD

11, 9643–9669, 2014

## Prediction of extreme floods based on CMIP5 climate models

C. H. Wu et al.

Title Page

Abstract

Introduction

Conclusions

References

Tables

Figures

⏪

⏩

◀

▶

Back

Close

Full Screen / Esc

Printer-friendly Version

Interactive Discussion



---

**Prediction of extreme floods based on CMIP5 climate models**C. H. Wu et al.

---

[Title Page](#)[Abstract](#)[Introduction](#)[Conclusions](#)[References](#)[Tables](#)[Figures](#)[⏪](#)[⏩](#)[◀](#)[▶](#)[Back](#)[Close](#)[Full Screen / Esc](#)[Printer-friendly Version](#)[Interactive Discussion](#)

basin, were used in this study. The GCMs data (precipitation and temperature) used include: (1) an historical simulation for the period 1970–2000 and (2) three new scenarios (RCP2.6, RCP4.5, and RCP8.5) for two different future periods (2020–2050 and 2050–2080). The model data and observations used in the study were interpolated to the same resolution on a  $0.25^\circ \times 0.25^\circ$  grid of the study area using bilinear interpolation. To reduce system errors in GCM simulations, the bias between the monthly precipitation and temperature of the observed and GCM output data was corrected using a quantile-based mapping method (Li et al., 2010). A stochastic weather generation method was then employed to temporally disaggregate the monthly downscaled climate projections into the daily weather forcings required by the hydrological model. To consider the range of variability that this randomness could induce, multiple downscaling simulations were performed for each projection (Raff et al., 2009). The simulation set size of this study was arbitrarily set to ten simulations.

## 2.4 Methodology

Variable Infiltration Capacity (VIC) model developed by Liang et al. (1994) is a macro-scale physical hydrological model based on a spatial distribution grid. It can simulate the physical exchange of water and energy among the soil, vegetation, and atmosphere in a surface vegetation-atmospheric transfer scheme (Wang et al., 2012). Further detailed information relating to the VIC can be obtained from University of Washington's website (<http://www.hydro.washington.edu/Lettenmaier/Models/VIC/SourceCode/Download.shtml>). As a typical land surface hydrological model, the VIC model has been successfully applied to assess the impact of climate change on hydrology over the Zhujiang River basin (Wu et al., 2014; Xiao et al., 2013). In this study, the model VIC 4.1.2b is used to simulate only the water balance, and is run over a regional domain consisting of 69 grid points at a spatial resolution of  $0.25^\circ \times 0.25^\circ$ .

The Mann–Kendall trend test (Mann, 1945; Kendall, 1975) is a nonparametric method to detect the significance of monotonic trends in hydrometeorological series (Wu et al., 2013a). In this study, we apply the Mann-Kendall method to detect statis-

tical significance of trends in future streamflow series as projected by GCMs. Here, two styles of trends tested are considered: trends tested without considering a level of significance and statistically significant trends at the 0.1 level.

The qualifier of “likelihood”, which provides calibrated language for describing quantified uncertainty, can be used to express a probabilistic estimate of the occurrence of a single event or of an outcome (IPCC, 2013). In this study, a total of 50 simulations for each projection of five GCMs were considered as a whole, and then likelihood terms associated with outcomes were defined as (IPCC, 2013):

Very likely: 90–100 %; Likely: 66–90 %; More likely than not: 50–66 %; About as likely as not: 33–50 %; Unlikely: 10–33 %; Very unlikely: 0–10 %.

We also use the qualifier “very likely” when, for example, the percentage of samples for one emission scenario shows increasing or decreasing trends of up to 90 %, we conclude that this trend (either increasing or decreasing) is “very likely” to occur.

### 3 Results and analysis

#### 3.1 VIC model validation

Observed forcing data required by VIC model were generated based on 27 rainfall stations with daily precipitation data, and 4 temperature stations with daily maximum and minimum temperatures data. The recorded data series was divided into two periods: the period 1969–1990 for model calibration and the period 1991–1999 for model validation. The efficacy of the simulation results was evaluated using the Nash–Sutcliffe efficiency coefficient (NSE) and relative error (RE).

As shown in Fig. 2a, the values of the NSE for the calibration and validation stages are 0.88 and 0.91, respectively, while the values of the RE are 11.88 and 3.67 %, respectively. The VIC model is accurate in simulating daily stream flow, with a high simulation precision of the flood peak in the flood season. In addition, VIC is also successful at simulating maximum 1-day and 7-day runoff depths, with high correlation coefficients

## Prediction of extreme floods based on CMIP5 climate models

C. H. Wu et al.

Title Page

Abstract

Introduction

Conclusions

References

Tables

Figures



Back

Close

Full Screen / Esc

Printer-friendly Version

Interactive Discussion



above 0.95 (Fig. 2b and c). These results indicate that the model has a good performance in simulating both daily stream flow and extreme floods in the selected catchment, and can therefore be used to estimate the potential impacts of climate change on floods.

### 3.2 Comparison of GCM simulations with observations

To assess the performance of the downscaling outputs from GCMs in simulating extreme precipitation, we compared the Empirical Cumulative Distribution Functions (ECDFs) of simulated maximum 1-day and 7-day precipitation (AMX1p and AMX7p, respectively) against the corresponding observations (Fig. 3a and b). The ECDFs of the ten simulations for each GCM are able to encompass a relatively wide distribution of AMX1p and AMX7p. In terms of the five models, BCC-CSM1.1 and MPI-ESM-LR perform better than the others, but there are relatively large differences between the performances of all the models. For example, CanESM2 underestimates AMX1p for non-exceedance probabilities up to approximately 0.8, and underestimates AMX7p for non-exceedance probabilities up to approximately 1.0. In addition, some models have a tendency to overestimate maximum values. For example in the case of CSIRO-Mk3.6.0, the tail of the distribution of projection-driven extreme precipitation begins to deviate significantly at the non-exceedance probability of approximately 0.9 to 1.0. Nevertheless, overall the five GCMs are able to simulate the range of extreme precipitation variability.

### 3.3 Evaluation of flood simulations by GCMs

This section is devoted to an evaluation of the flood simulation ability of each GCM based on the VIC model driven by historical resampling. Figure 3c and d show the ECDFs of observed and simulated annual maximum 1-day discharges (AMX1d) and maximum 7-day flood volumes (AMX7fv) at the Hengshi hydrologic station during the period 1970–2000.

Title Page

Abstract

Introduction

Conclusions

References

Tables

Figures

⏪

⏩

◀

▶

Back

Close

Full Screen / Esc

Printer-friendly Version

Interactive Discussion



Compared to the Fig. 3a and b, it can be seen that the frequency distribution of extreme floods is very similar to that of precipitation. In contrast, results from individual model ensembles show different characteristics. For example, an overestimation of floods is present in CSIRO-Mk3.6.0, while an underestimation of floods is found in CanESM2 and GISS-E2-R; such differences can be explained by the patterns of temperature and precipitation behavior in each model. However, overall, the simulation sequences from the five GCMs proficiently capture the observed historical extreme floods in the study catchment (five GCMs simulation in Fig. 3c and d); the uncertainty range for changes in flood magnitude is well-represented by the five GCMs as a whole.

### 3.4 Trend analysis for extreme floods in future periods

To understand the trends in projected extreme flood events, the Mann–Kendall method was used to test the presence of monotonic trends in the AMX1d and AMX7fv sequences in two different future periods (Fig. 4). Overall, the range in the number of samples for AMX1d and AMX7fv has very similar characteristics during both future periods. Furthermore, the samples projected by the five GCMs mostly show increasing trends over the two future periods, but rarely show significant trends at the 0.1 level. GCMs are often considered to produce a large uncertainty in predictions of future floods, and as expected, there is a difference in projected trends over the study area from the different GCMs. Using the RCP4.5 scenario for example, only one sample of AMX1d experiences increasing trends in the BCC-CSM1.1 and MPI-ESM-LR models during the period 2020–2050. However, five samples with increasing trends can be found in the CanESM2 and GISS-E2-R models, and ten samples in the CSIRO-Mk3.6.0 model. Additionally, the uncertainty produced by the emission scenarios is also large here. For the same GCM, the number of samples with increasing trends varies from scenario to scenario. If we examine the BCC-CSM1.1 model for example, there is an increasing trend for nine samples of AMX1d and AMX7fv during the period 2020–2050 under the RCP2.6 scenario, but for only one sample under the RCP4.5 scenario, and then for five samples under the RCP8.5 scenario.

[Title Page](#)

[Abstract](#)

[Introduction](#)

[Conclusions](#)

[References](#)

[Tables](#)

[Figures](#)

[⏪](#)

[⏩](#)

[◀](#)

[▶](#)

[Back](#)

[Close](#)

[Full Screen / Esc](#)

[Printer-friendly Version](#)

[Interactive Discussion](#)





nario in 2020–2050, the maximum value of AMX1d projected by CanESM2 is less than  $18\,000\text{ m}^3\text{ s}^{-1}$ , whereas the maximum value of AMX1d projected by CSIRO-Mk3.6.0 even exceeds  $42\,000\text{ m}^3\text{ s}^{-1}$ . In addition, overall, the largest and smallest ranges of AMX1d and AMX7fv are projected by CSIRO-Mk3.6.0 and GISS-E2-R, respectively.

Compared to the baseline period 1970–2000, the boxes in Fig. 5 are located in the higher position for most future scenarios of five GCMs, especially for BCC-CSM1.1 and MPI-ESM-LR. This means that the possibility of a projected increase in extreme floods is bigger than that of a projected decrease. When comparing two different future periods, it can be found that the projected changes in 2050–2080 would be larger than those in 2020–2050 for most of future scenarios.

### 3.6 Average changes in extreme floods in future periods

Based on ten simulations for each emission scenario, the average changes in extreme floods for each future scenario are analysed in this section. Here, the “average” for each future scenario is the arithmetic average of ten simulations. To compare the frequency of extreme floods between baseline and future periods, P-III frequency distributions are plotted for comparison (Fig. 6). When the frequency is less than 10%, most of future scenarios of the five models suggest a rather similar increasing trend in AMX1d and AMX7fv, where the largest projected increases (absolute change) are found for the CSIRO-Mk3.6.0 model, and the smallest increases for the GISS-E2-R model. In terms of two different future periods, the projected increases in 2050–2080 are larger than those in 2020–2050 for most future scenarios. In particular, the BCC-CSM1.1 model projects a maximum increase ( $p < 10\%$ ) in AMX1d and AMX7fv for the RCP4.5 and RCP8.5 scenarios during 2050–2080 and a minimum increase for the RCP2.6 scenario during 2020–2050. For the CanESM2 model, a maximum increase ( $p < 10\%$ ) is found for the RCP4.5 scenario during 2020–2050, while the opposite tendency (decrease) is found for the RCP2.6 scenario during both 2020–2050 and 2050–2080. CSIRO-Mk3.6.0 projects a large increase in AMX1d and AMX7fv for the RCP2.6 scenario during 2020–2050 and for the RCP8.5 scenario in 2050–2080, but projects a

Title Page

Abstract

Introduction

Conclusions

References

Tables

Figures



Back

Close

Full Screen / Esc

Printer-friendly Version

Interactive Discussion







## Prediction of extreme floods based on CMIP5 climate models

C. H. Wu et al.

[Title Page](#)

[Abstract](#)

[Introduction](#)

[Conclusions](#)

[References](#)

[Tables](#)

[Figures](#)

[⏪](#)

[⏩](#)

[◀](#)

[▶](#)

[Back](#)

[Close](#)

[Full Screen / Esc](#)

[Printer-friendly Version](#)

[Interactive Discussion](#)



In addition, when using a hydrological model to assess the impact of climate change, there is an implicit assumption that the hydrological model parameters calibrated from observations remain valid for future climatic conditions (Xu et al., 2013). However, Merz et al. (2011) pointed that hydrological model parameters may potentially change if calibrated to different periods, and such a concept has important implications in climate impact analyses. Therefore, a next step of this study is a thorough investigation of the uncertainty produced by hydrological model (VIC) structure and its parameters in the projection of impact of climate change on floods.

To highlight the uncertainty of the results, this paper attempts to describe the credibility of projected flood changes with an approach using uncertainty expressions, as recommended by the AR5. This provides a quantitative basis for estimating likelihoods for many aspects of future climate change. However, the results should be taken with care, as the likelihood scheme itself is inappropriate for use in subjective evaluation and needs to be supplemented with a qualitative framework (Risbey and Kandlikar, 2007). Use of a best combination of levels of confidence with likelihood, which provides more powerful means for analysts to express uncertainty, should be considered in future work.

## 5 Conclusions

Based on five CMIP5 GCMs, this paper discusses the potential impacts of climate change on extreme floods in the Beijiing River basin. Two flood indexes (AMX1d and AMX7fv) were chosen for use in analysis, and uncertainty in future flood trends was considered by using an uncertainty expressions approach.

Modeling results indicate that there are large uncertainties sourced from GCMs and emission scenarios. Overall, the uncertainty range for changes in historical extreme precipitation and flood magnitude can be well represented by the five GCMs. The largest possibilities of increasing trends in AMX1d and AMX7fv were found for the RCP2.6 scenario during the two future periods, whereas the smallest possibilities of in-



## Prediction of extreme floods based on CMIP5 climate models

C. H. Wu et al.

[Title Page](#)

[Abstract](#)

[Introduction](#)

[Conclusions](#)

[References](#)

[Tables](#)

[Figures](#)

[⏪](#)

[⏩](#)

[◀](#)

[▶](#)

[Back](#)

[Close](#)

[Full Screen / Esc](#)

[Printer-friendly Version](#)

[Interactive Discussion](#)



Hansen, M. C., Defries, R. S., Townshend, J. R. G., and Sohlberg, R.: Global land cover classification at 1 km spatial resolution using a classification tree approach, *Int. J. Remote Sens.*, 21, 1331–1364, 2000.

Huang, S., Hattermann, F. F., Krysanova, V., and Bronstert, A.: Projections of climate change impacts on river flood conditions in Germany by combining three different RCMs with a regional eco-hydrological model, *Clim. Change*, 116, 631–663, 2013.

IPCC: Climate Change 2013: The Physical Science Basis. Contribution of Working Group I to the Fifth Assessment Report of the Intergovernmental Panel on Climate Change, edited by: Stocker, T. F., Qin, D., Plattner, G.-K., Tignor, M., Allen, S. K., Boschung, J., Nauels, A., Xia, Y., Bex, V., and Midgley, P. M., Cambridge University Press, Cambridge, United Kingdom and New York, NY, USA, 1535 pp., 2013.

Kay, A. L., Davies, H. N., Bell, V. A., and Jones, R. G.: Comparison of uncertainty sources for climate change impacts: flood frequency in England, *Clim. Change*, 92, 41–63, 2009.

Kay, A. L. and Jones, D. A.: Transient changes in flood frequency and timing in Britain under potential projections of climate change, *Int. J. Climatol.*, 32, 489–502, 2012.

Kendall, M. G.: Rank Correlation Methods, 4th edn. Charles Griffin: London, UK, 1–202, 1975.

Li, H., Sheffield, J., and Wood, E. F.: Bias correction of monthly precipitation and temperature fields from Intergovernmental Panel on Climate Change AR4 models using equidistant quantile matching, *J. Geophys. Res.-Atmos.*, 115, D10101, doi:10.1029/2009JD012882, 2010.

Liang, X., Lettenmaier, D. P., Wood, E. F., and Burges, S. J.: A simple hydrologically based model of land surface water and energy fluxes for general circulation models, *J. Geophys. Res.-Atmos.*, 99, 14415–14428, 1994.

Liu, L. L., Fischer, T., Jiang, T., and Luo, Y.: Comparison of uncertainties in projected flood frequency of the Zhujiang River, South China, *Quatern. Int.*, 304, 51–61, 2013.

Mann, H. B.: Non-Parametric tests against trend, *Econometrica*, 13, 245–259, 1945.

Merz, R., Parajka, J., and Blöschl, G.: Time stability of catchment model parameters: Implications for climate impact analyses, *Water Resour. Res.*, 47, W02531, doi:10.1029/2010WR009505, 2011.

Mirza, M. M. Q., Warrick, R. A., and Ericksen, N. J.: The implications of climate change on floods of the Ganges, Brahmaputra and Meghna rivers in Bangladesh, *Clim. Change*, 57, 287–318, 2003.

Moss, R. H., Edmonds, J. A., Hibbard, K. A., Manning, M. R., Rose, S. K., van Vuuren, D. P., Carter, T. R., Emori, S., Kainuma, M., Kram, T., Meehl, G. A., Mitchell, J. F. B., Nakicenovic,

## Prediction of extreme floods based on CMIP5 climate models

C. H. Wu et al.

[Title Page](#)

[Abstract](#)

[Introduction](#)

[Conclusions](#)

[References](#)

[Tables](#)

[Figures](#)

[⏪](#)

[⏩](#)

[◀](#)

[▶](#)

[Back](#)

[Close](#)

[Full Screen / Esc](#)

[Printer-friendly Version](#)

[Interactive Discussion](#)



N., Riahi, K., Smith, S. J., Stouffer, R. J., Thomson, A. M., Weyant, J. P., and Wilbanks, T. J.: The next generation of scenarios for climate change research and assessment, *Nature*, 463, 747–756, 2010.

Pennell, C. and Thomas, R.: On the Effective Number of Climate Models, *J. Clim.*, 24, 2358–2367, 2011.

Pierce, D. W., Westerling, A. L., and Oyster, J.: Future humidity trends over the western United States in the CMIP5 global climate models and variable infiltration capacity hydrological modeling system, *Hydrol. Earth Syst. Sci.*, 17, 1833–1850, doi:10.5194/hess-17-1833-2013, 2013.

Pincus, R., Batstone, C. P., Hofmann, R. J. P., Taylor, K. E., and Glecker, P. J.: Evaluating the present-day simulation of clouds, precipitation, and radiation in climate models, *J. Geophys. Res.-Atmos.*, 113, D14209, doi:10.1029/2007JD009334, 2008.

Prudhomme, C. and Davies, H. N.: Assessing uncertainties in climate change impact analyses on river flow regimes in the UK. Part 2: future climate, *Clim. Change*, 93, 197–222, 2009.

Raff, D. A., Pruitt, T., and Brekke, L. D.: A framework for assessing flood frequency based on climate projection information, *Hydrol. Earth Syst. Sci.*, 13, 2119–2136, doi:10.5194/hess-13-2119-2009, 2009.

Risbey, J. S. and Kandlikar, M.: Expressions of likelihood and confidence in the IPCC uncertainty assessment process, *Clim. Change*, 85, 19–31, 2007.

Sachindra, D. A., Huang, F., Barton, A., and Perera, B. J. C.: Statistical downscaling of general circulation model outputs to precipitation—part 1: calibration and validation, *Int. J. Climatol.*, doi:10.1002/joc.3914, in press, 2014a.

Sachindra, D. A., Huang, F., Barton, A., and Perera, B. J. C.: Statistical downscaling of general circulation model outputs to precipitation—part 2: bias-correction and future projections, *Int. J. Climatol.*, doi:10.1002/joc.3915, in press, 2014b.

Smith, I., Syktus, J., McAlpine, C., and Wong, K.: Squeezing information from regional climate change projections—results from a synthesis of CMIP5 results for south-east Queensland, Australia, *Clim. Change*, 121, 609–619, 2013.

Taylor, K. E., Stouffer, R. J., and Meehl, G. A.: An Overview of CMIP5 and the Experiment Design, *B. Am. Meteorol. Soc.*, 93, 485–498, 2012.

Teng, J., Vaze, J., Chiew, F. H. S., Wang, B., and Perraud, J.: Estimating the Relative Uncertainties Sourced from GCMs and Hydrological Models in Modeling Climate Change Impact on Runoff, *J. Hydrometeorol.*, 13, 122–139, 2012.

## Prediction of extreme floods based on CMIP5 climate models

C. H. Wu et al.

Title Page

Abstract

Introduction

Conclusions

References

Tables

Figures

⏪

⏩

◀

▶

Back

Close

Full Screen / Esc

Printer-friendly Version

Interactive Discussion



Tisseuil, C., Vrac, M., Lek, S., and Wade, A. J.: Statistical downscaling of river flows, *J. Hydrol.*, 385, 279–291, 2010.

Wang, G. Q., Zhang, J. Y., Jin, J. L., Pagano, T. C., Calow, R., Bao, Z. X., Liu, C. S., Liu, Y. L., and Yan, X. L.: Assessing water resources in China using PRECIS projections and a VIC model, *Hydrol. Earth Syst. Sci.*, 16, 231–240, doi:10.5194/hess-16-231-2012, 2012.

Wu, C. H., Huang, G. R., Yu, H. J., Chen, Z. Q., and Ma, J. G.: Spatial and temporal distributions of trends in climate extremes of the Feilaixia catchment in the upstream area of the Beijiing River Basin, South China, *Int. J. Climatol.*, doi:10.1002/joc.3900, in press, 2013a.

Wu, Z. Y., Lu, G. H., Liu, Z. Y., Wang, J. X., and Xiao, H.: Trends of Extreme Flood Events in the Pearl River Basin during 1951–2010, *Adv. Climate Change Res.*, 4, 110–116, 2013b.

Wu, C., Huang, G., Yu, H., Chen, Z., and Ma, J.: Impact of climate change on reservoir flood control in the upstream area of the Beijiing River Basin, South China, *J. Hydrometeor.*, doi:10.1175/JHM-D-13-0181.1, in press, 2014.

Xiao, H., Lu, G. H., Wu, Z. Y., and Liu Z. Y.: Flood response to climate change in the Pearl River basin for the next three decades, *J. Hydraul. Eng.*, 12, 1409–1419, 2013 (in Chinese).

Xu, Y. P., Zhang, X., Ran, Q., and Tian, Y.: Impact of climate change on hydrology of upper reaches of Qiantang River Basin, East China, *J. Hydrol.*, 483, 51–60, 2013.

## Prediction of extreme floods based on CMIP5 climate models

C. H. Wu et al.

[Title Page](#)

[Abstract](#)

[Introduction](#)

[Conclusions](#)

[References](#)

[Tables](#)

[Figures](#)

[⏪](#)

[⏩](#)

[◀](#)

[▶](#)

[Back](#)

[Close](#)

[Full Screen / Esc](#)

[Printer-friendly Version](#)

[Interactive Discussion](#)



**Table 1.** Percentage of samples with increasing trends of AMX1d and AMX7fv in future periods based on five GCMs.

Flood index	Emissions scenarios	2020–2050		2050–2080	
		IT	SIT	IT	SIT
AMX1d	RCP2.6	60	10	74	10
	RCP4.5	44	2	38	2
	RCP8.5	54	2	72	8
AMX7fv	RCP2.6	60	8	68	10
	RCP4.5	44	2	44	0
	RCP8.5	58	2	62	10

IT, Increasing Trend. SIT, Significant Increasing Trend (significant at the 0.1 level).

**Table 2.** Percentage changes (%) in AMX1d and AMX7fv under different scenarios (relative to the baseline period 1970–2000).

Flood index	Return period (a)	GCM	RCP2.6		RCP4.5		RCP8.5	
			T1	T2	T1	T2	T1	T2
AMX1d	500	BCC-CSM1.1	17.7	47	43.3	69.5	50.9	58.3
		CanESM2	-11.2	-2.7	118	49.9	28.8	22.5
		CSIRO-Mk3.6.0	41.3	2.2	-16.2	14.7	7.4	85.3
		GISS-E2-R	24.7	36.5	-0.2	18.8	-5.8	19.3
	MPI-ESM-LR	21.5	3.8	47.3	51.2	15	28.1	
	200	BCC-CSM1.1	14.3	43.3	40	66	44.9	53.6
		CanESM2	-9.7	-1.9	103.3	46	26.8	21
		CSIRO-Mk3.6.0	36.5	4.2	-13.6	16.6	7.7	79.8
		GISS-E2-R	21.9	30.6	-0.4	15.1	-7.1	15.8
	MPI-ESM-LR	17.9	2.9	41.6	45.9	12.4	25.3	
	100	BCC-CSM1.1	11.4	40.2	37.1	62.9	39.8	49.6
		CanESM2	-8.5	-1.2	91	42.7	25.2	19.7
CSIRO-Mk3.6.0		32	6	-11.3	18.2	8	74.7	
GISS-E2-R		19.5	25.7	-0.5	12	-8.2	12.8	
MPI-ESM-LR	15	2.1	36.8	41.3	10.3	23		
50	BCC-CSM1.1	8.3	36.6	33.9	59.3	34.1	45.1	
	CanESM2	-7.1	-0.4	77.4	39	23.3	18.4	
	CSIRO-Mk3.6.0	26.7	8.1	-8.5	20.2	8.2	68.4	
	GISS-E2-R	16.8	20.5	-0.5	8.7	-9.4	9.6	
MPI-ESM-LR	11.9	1.3	31.5	36.3	8	20.4		
AMX7fv	500	BCC-CSM1.1	14.2	61.8	44.4	64.5	35.9	73.1
		CanESM2	-6.9	-5.2	103.7	59	38.3	35.7
		CSIRO-Mk3.6.0	39	-3.5	-22.7	10.3	8.3	81.5
		GISS-E2-R	19	43	1.7	28.7	-3.2	14.9
	MPI-ESM-LR	16.2	6	56.6	58.6	18.5	28.7	
	200	BCC-CSM1.1	11.2	55.5	39.7	61	31.4	64.7
		CanESM2	-6	-3.9	90.8	53.9	34.7	32.2
		CSIRO-Mk3.6.0	34.4	-0.7	-19.6	12.9	8.7	76.5
		GISS-E2-R	16.6	35.6	1.3	23.2	-5.2	12.2
	MPI-ESM-LR	14.1	4.6	49.1	51.2	15.1	25.6	
	100	BCC-CSM1.1	8.6	50.3	35.8	58.1	27.6	57.8
		CanESM2	-5.2	-2.9	80.1	49.5	31.6	29.2
CSIRO-Mk3.6.0		30.2	1.8	-16.8	15.2	9	71.8	
GISS-E2-R		14.5	29.5	0.9	18.7	-6.8	9.8	
MPI-ESM-LR	12.4	3.4	42.9	45.2	12.2	23		
50	BCC-CSM1.1	5.9	44.4	31.5	54.7	23.5	50.3	
	CanESM2	-4.2	-1.7	68.5	44.7	28.2	26.1	
	CSIRO-Mk3.6.0	25.1	4.8	-13.4	18	9.3	66	
	GISS-E2-R	12.3	23.1	0.6	13.9	-8.4	7.3	
MPI-ESM-LR	10.6	2.2	36.1	38.6	9.2	20		

T1, 2020–2050; T2, 2050–2050.

Title Page

Abstract Introduction

Conclusions References

Tables Figures

⏪ ⏩

⏴ ⏵

Back Close

Full Screen / Esc

Printer-friendly Version

Interactive Discussion



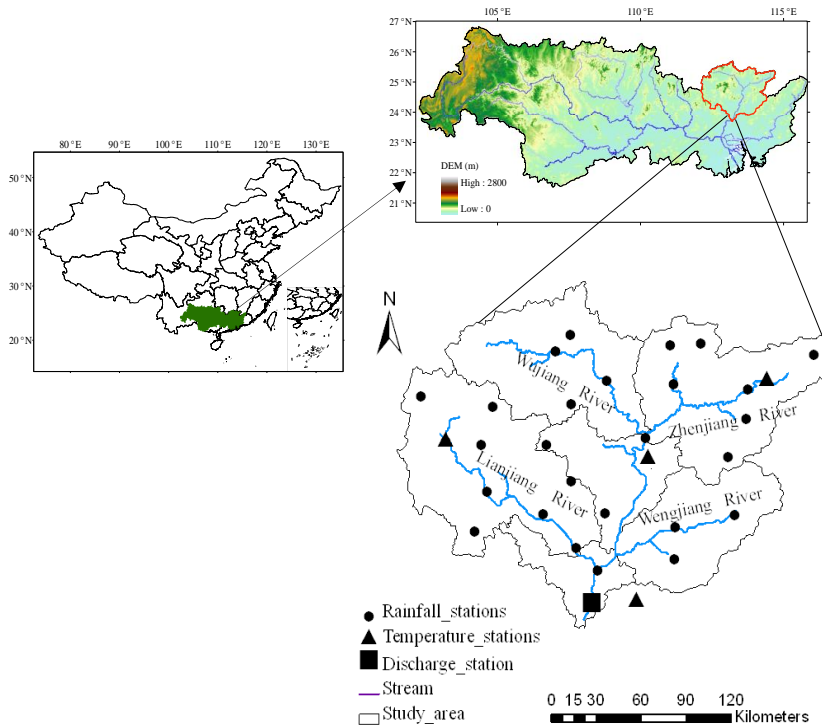


**Figure 1.** Map showing the location of study catchment.

## Prediction of extreme floods based on CMIP5 climate models

C. H. Wu et al.

[Title Page](#)

[Abstract](#)

[Introduction](#)

[Conclusions](#)

[References](#)

[Tables](#)

[Figures](#)

[⏪](#)

[⏩](#)

[◀](#)

[▶](#)

[Back](#)

[Close](#)

[Full Screen / Esc](#)

[Printer-friendly Version](#)

[Interactive Discussion](#)



## Prediction of extreme floods based on CMIP5 climate models

C. H. Wu et al.

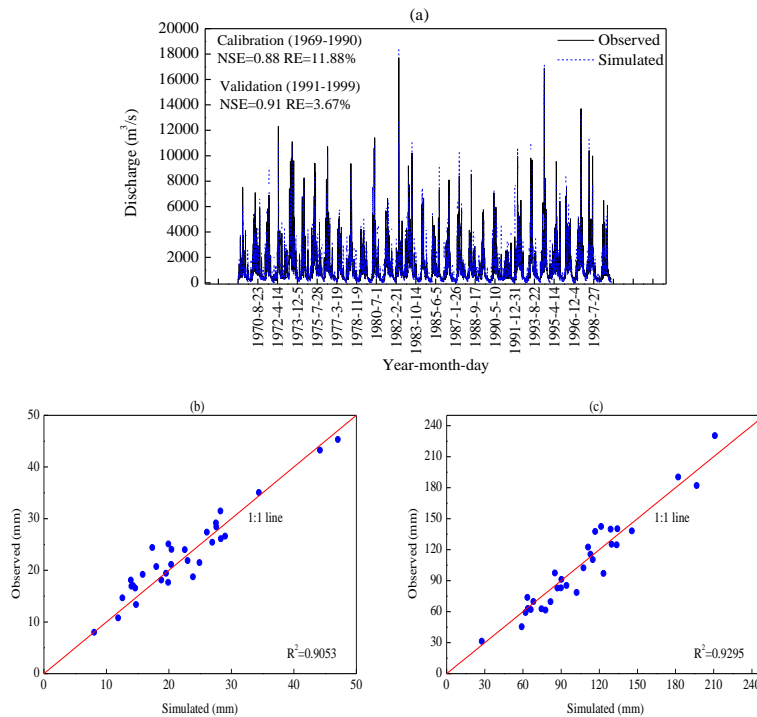


**Figure 2.** Comparison of the simulated and observed runoff during the period 1969–1999. **(a)** A comparison of simulated and observed discharges; **(b)** a comparison of simulated and observed maximum 1-day runoff depth and **(c)** a comparison of simulated and observed maximum 7-day runoff depth.

[Title Page](#)
[Abstract](#)
[Introduction](#)
[Conclusions](#)
[References](#)
[Tables](#)
[Figures](#)
[Back](#)
[Close](#)
[Full Screen / Esc](#)
[Printer-friendly Version](#)
[Interactive Discussion](#)

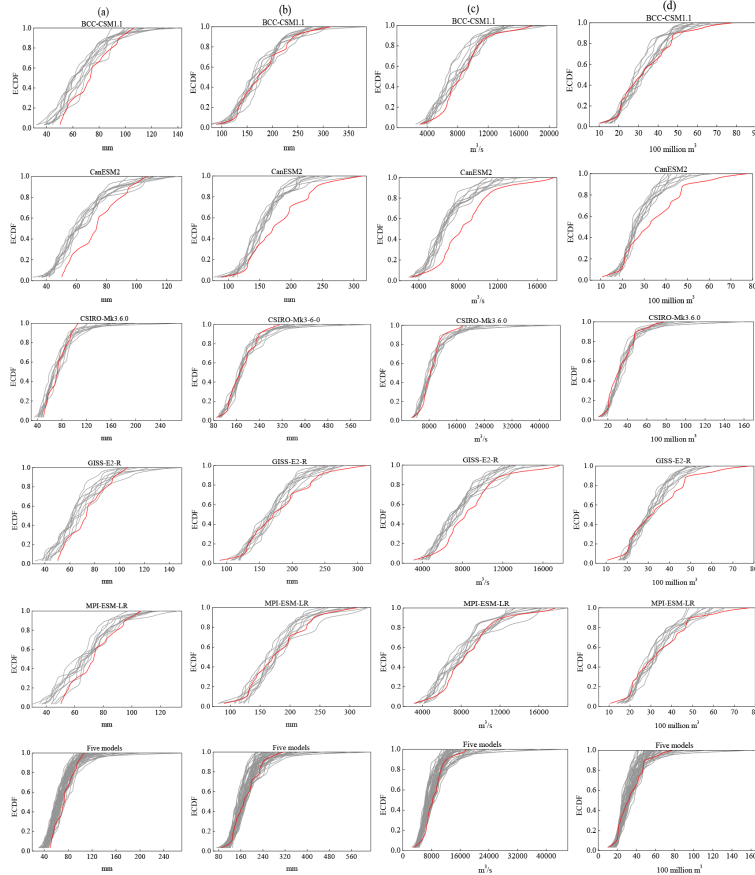


**Figure 3.** ECDFs for observed and simulated (a) AMX1p, (b) AMX7p, (c) AMX1d and (d) AMX7fv during the period 1970–2000. Red line represents the observed. Grey lines represent ensemble of projections.

**Prediction of extreme floods based on CMIP5 climate models**

C. H. Wu et al.

Title Page

Abstract	Introduction
Conclusions	References
Tables	Figures

⏪
⏩

◀
▶

Back	Close
------	-------

Full Screen / Esc

Printer-friendly Version

Interactive Discussion



## Prediction of extreme floods based on CMIP5 climate models

C. H. Wu et al.

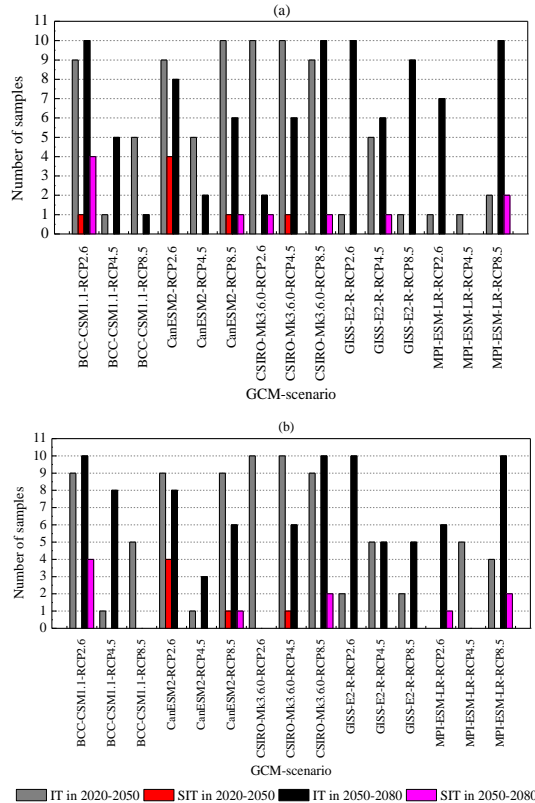


**Figure 4.** Number of the samples with increasing trends for **(a)** AMX1d and **(b)** AMX7fv under different scenarios. IT indicates increasing trend. SIT indicates significant increasing trend at the 0.1 level.

[Title Page](#)

[Abstract](#) | [Introduction](#)

[Conclusions](#) | [References](#)

[Tables](#) | [Figures](#)

[◀](#) | [▶](#)

[◀](#) | [▶](#)

[Back](#) | [Close](#)

[Full Screen / Esc](#)

[Printer-friendly Version](#)

[Interactive Discussion](#)



## Prediction of extreme floods based on CMIP5 climate models

C. H. Wu et al.

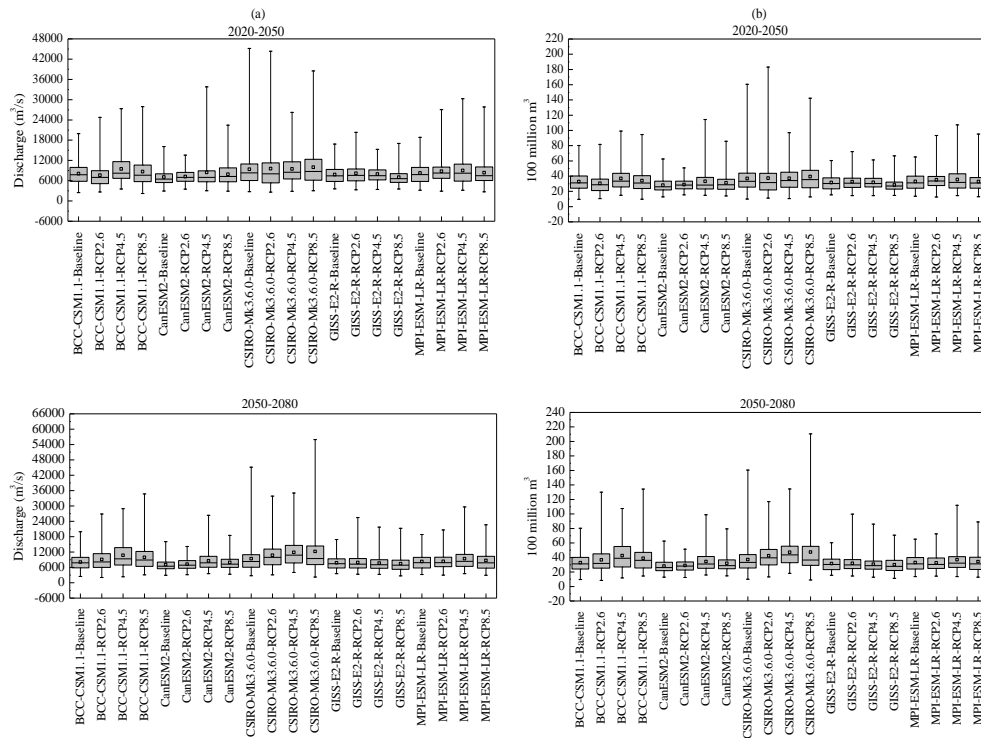


**Figure 5.** Uncertainty range of (a) AMX1d and (b) AMX7fv under different scenarios. Box plots: the central mark is the median; the small square inside the box is the average; the box-edges are the 25th and 75th percentiles; the whiskers extend to the 1st and 99th percentiles.

[Title Page](#)

[Abstract](#)

[Introduction](#)

[Conclusions](#)

[References](#)

[Tables](#)

[Figures](#)



[Back](#)

[Close](#)

[Full Screen / Esc](#)

[Printer-friendly Version](#)

[Interactive Discussion](#)



## Prediction of extreme floods based on CMIP5 climate models

C. H. Wu et al.

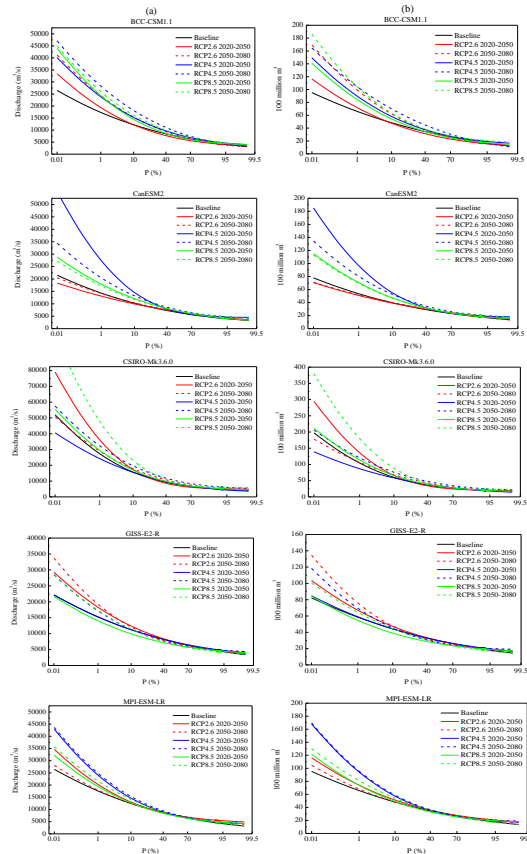


**Figure 6.** P-III frequency distributions of **(a)** AMX1d and **(b)** AMX7iv under different scenarios during two different future periods.

Title Page

Abstract	Introduction
Conclusions	References
Tables	Figures

⏪      ⏩  
⏴      ⏵  
Back      Close

Full Screen / Esc

Printer-friendly Version

Interactive Discussion

